Direct Interaction of the Inhibitory γ-Subunit of Rod cGMP Phosphodiesterase (PDE6) with the PDE6 GAFa Domains†

Khakim G. Muradov,‡ Alexey E. Granovsky,‡ Kevin L. Schey,§ and Nikolai O. Artemyev*,‡

Department of Physiology and Biophysics, University of Iowa College of Medicine, Iowa City, Iowa 52242, and Department of Pharmacology, Medical University of South Carolina, Charleston, South Carolina 29403

Received November 13, 2001; Revised Manuscript Received December 27, 2001

ABSTRACT: Retinal rod and cone cGMP phosphodiesterases (PDE6 family) function as the effector enzyme in the vertebrate visual transduction cascade. The activity of PDE6 catalytic subunits is controlled by the Pγ-subunits. In addition to the inhibition of cGMP hydrolysis at the catalytic sites, Pγ is known to stimulate a noncatalytic binding of cGMP to the regulatory GAFa−GAFb domains of PDE6. The latter role of Pγ has been attributed to its polycationic region. To elucidate the structural basis for the regulation of cGMP binding to the GAF domains of PDE6, a photoexcitable peptide probe corresponding to the polycationic region of Pγ, Pγ-21−45, was specifically cross-linked to rod PDE6αβ. The site of Pγ-21−45 cross-linking was localized to Met[138]Gly[139] within the PDE6α GAFa domain using mass spectrometric analysis. Chimeras between PDE5 and cone PDE6α′, containing GAFa and/or GAFb domains of PDE6α′ have been generated to probe a potential role of the GAFb domains in binding to Pγ. Analysis of the inhibition of the PDE5/PDE6α′ chimeras by Pγ supported the role of PDE6 GAFa but not GAFb domains in the interaction with Pγ. Our results suggest that a direct binding of the polycationic region of Pγ to the GAFa domains of PDE6 may lead to a stabilization of the noncatalytic cGMP-binding sites.

Photoreceptor rod and cone cGMP phosphodiesterases (PDE6)[1] are the effector enzymes in the vertebrate visual transduction cascade. Rod PDE6 is a catalytic heterodimer composed of the homologous PDE6 α- and β-subunits. Each PDE6 catalytic subunit has a copy of the tightly bound γ-subunit (Pγ) that blocks cGMP hydrolysis at the active sites. The enzyme activity is drastically stimulated when photoexcited rhodopsin induces GTP/GDP exchange on the visual G protein, transducin (Gt), and GtαGTP displaces Pγ from the inhibitory sites on PDE6 catalytic subunits (*1*, *2*). Cone PDE6, which consists of a catalytic homodimer PDE6α′ and two copies of cone-specific Pγ subunit, is structurally and functionally homologous to rod PDE6 (*3*−*5*). Conserved catalytic domains are located within the C-terminal half of the PDE6 catalytic subunits. The N-terminal domains of PDE6 catalytic subunits contain two sites, a and b, for noncatalytic binding of cGMP (*4*). Although each PDE6 catalytic dimer has four noncatalytic cGMP-binding motifs, the maximal stoichiometry of only 2 mol of cGMP/mol of PDE6 dimer has been reported (*6*−*9*). The PDE6 noncatalytic cGMP-binding regions are structurally dissimilar to those in cGMP-dependent protein kinase and cGMP-gated ion channels but homologous to structural motifs termed GAF domains (*10*−*12*). GAF domains are present in a large family of proteins including PDEs from the PDE families 2, 5, 8, 10, and 11 and various plant, fungal, and bacterial signaling and regulatory proteins (*11*). The functional significance of the PDE6 GAF domains in the visual transduction cascade is not well understood. Evidence suggests that the binding of Pγ to PDE6 catalytic subunits enhances the affinity of cGMP for the noncatalytic sites. Reciprocally, when the GAF domains are occupied with cGMP, the affinity of Pγ for the PDE6 catalytic subunits is greater (*9*, *13*−*15*). Despite a significant recent expansion of the structural information on the PDE6−Pγ interaction, the mechanism of positive cooperativity of the GAF domains and the Pγ-binding sites on PDE6 remains unknown. Two regions of the rod Pγ-subunit, the central polycationic domain, Pγ-24−45, and the C-terminal tail, roughly Pγ-75−87, constitute the major PDEαβ interaction domains (*16*−*19*). The C-terminus of Pγ is a key inhibitory domain. It interacts directly with the active site of PDE6 and occludes the catalytic cavity, thereby blocking cGMP hydrolysis (*20*−*22*). The polycationic region of Pγ was thought to serve primarily as a binding domain that increases the overall affinity of Pγ for PDE6 catalytic subunits (*16*−*19*). A new function of this domain had been revealed when we first demonstrated that it enhances the affinity of cGMP binding to the GAF domains of cone PDE6 (*8*). Recent study has shown that the polycationic region of Pγ restores high-affinity cGMP binding to the GAF domains of rod PDE (*9*). Furthermore, the binding affinity of Pγ-1−45 to PDE6αβ

† This work was supported by National Institutes of Health Grant EY-10843. N.O.A. is an Established Investigator of the American Heart Association. The services provided by the Diabetes and Endocrinology Research Center of the University of Iowa were supported by NIH Grant DK-25295. We acknowledge use of the Biological Mass Spectrometry Facility at the Medical University of South Carolina.

* To whom correspondence should be addressed. Tel: 319-335-7864. Fax: 319-335-7330. E-mail: nikolai-artemyev@uiowa.edu.

‡ University of Iowa College of Medicine.

§ Medical University of South Carolina.

[1] Abbreviations: PDE, cGMP phosphodiesterase; PDE6, photoreceptor PDE (PDE6 family); Pγ, γ-subunit of PDE6; PDE5, cGMP-binding, cGMP-specific PDE (PDE5 family); MALDI, matrix-assisted laser desorption ionization mass spectrometry.

10.1021/bi015935m CCC: $22.00
Published on Web 03/03/2002

was increased when the GAF domains were occupied by cGMP (*9*). Therefore, the polycationic region of Pγ appears to be responsible for the reciprocal relationships between Pγ and noncatalytic cGMP-binding sites.

In this study, we sought to identify the Pγ polycationic region binding site on PDE6 catalytic subunits to elucidate the structural basis for the reciprocal regulation of PDE6 by the γ-subunit and the GAF domains. A peptide probe corresponding to Pγ-21−45 was designed to incorporate a photoactivatable residue, benzoylphenylalanine. A site of specific cross-linking of the probe was identified as Met^{138}-Gly^{139} of the PDE6α subunit, suggesting a direct binding of Pγ-21−45 to the PDE6 GAFa domain. The role of PDE6 GAFa domains in the interaction with Pγ has been confirmed using chimeric PDE5/6 enzymes containing GAFa and/or GAFb from cone PDE6α′.

EXPERIMENTAL PROCEDURES

Preparation of HoloPDE6 and PDE6αβ. Bovine ROS membranes were prepared by the method of Papermaster and Dreyer (*23*). HoloPDE6 was extracted from bleached ROS membranes and concentrated by ultrafiltration using a YM-30 membrane (Amicon). Concentrated PDE extract was subjected to a limited proteolysis with trypsin to obtain PDE6αβ as described previously (*20*). This trypsin-treated PDE contained equimolar amounts of the 88 kDa PDE6α and N-terminally truncated 70 kDa PDE6β polypeptides (*20*). HoloPDE6 and PDE6αβ preparations were purified by ion-exchange FPLC on a MonoQ column (Pharmacia) to a purity greater than 95%, based on densitometric scanning of Coomassie Blue-stained gels (*20*).

Cross-Linking of Pγ-21−45Bpa^{23} to PDE6αβ and Isolation of Cross-Linked Fragments. A peptide, Btn-NH-$(CH_2)_5$-CO-^{21}VT*Bpa*RKGPPKFKQRQTRQFKSKPPKK^{45}-NH_2 (Pγ-21−45Bpa^{23}), corresponding to residues 21−45 of bovine rod Pγ was custom made by Genosys Biotechnologies Inc. *p*-Benzoyl-L-phenylalanine (Bpa), a photoexcitable cross-linking probe, was incorporated instead of PγPro^{23}. The peptide was biotinylated at the N-terminus using biotin−aminohexanoic acid and amidated at the C-terminus. In a typical experiment, PDE6αβ (2 μM) was mixed with Pγ-21−45Bpa^{23} (10 μM) in 20 mM HEPES (pH 7.5) buffer containing 100 mM NaCl and 4 mM $MgSO_4$ and incubated on ice for 20 min. The samples were then UV-irradiated in a polypropylene tube at a distance of 1 cm for 2 min using a UV Transilluminator lamp (UVP, Upland, CA). The mixture was centrifuged (70000*g*, 30 min), and the supernatant was loaded into a C4 214TP54 reversed-phase HPLC column (Vydac) to separate PDE6αβ/Pγ-21−45Bpa^{23} cross-linked products from the free peptide. A HPLC fraction containing PDE6αβ/Pγ-21−45Bpa^{23} cross-linked products was dried using SpeedVac and digested with pepsin (a protein/pepsin weight/weight ratio 20:1) in 30 mM HCl solution for 6 h at 25 °C. The biotin-containing cross-linked peptides were purified using an UltraLink immobilized monomeric avidin resin (Pierce). To block nonreversible biotin-binding sites, the resin was incubated with a 0.15 mM solution of D-biotin and washed with 0.2 M glycine (pH 2.8). A monomeric avidin resin (10 μL) was equilibrated with 30 mM Tris-HCl (pH 7.5) buffer containing 500 mM NaCl in a tip column. The pepsin digest with pH adjusted to 7.5 was loaded onto the resin, which was then washed with the equilibrating buffer. The bound biotin-containing peptides were eluted with 0.2 M glycine (pH 2.8) and applied onto a C18 218TP54 reversed-phase HPLC column (Vydac). Biotin-containing HPLC fractions were identified using dot blot and Western blot analyses with a streptavidin/horseradish peroxidase conjugate detection and dried using a SpeedVac. Dried HPLC fractions were solubilized in 10% acetonitrile/50 mM ammonium bicarbonate, pH 8.5 (20 μL), and digested with trypsin (20 ng) at 37 °C overnight.

Identification of PDE6αβ/Pγ-21−45Bpa^{23} Cross-Linked Fragments by Mass Spectrometry. Pepsin and pepsin plus trypsin products were analyzed by matrix-assisted laser desorption ionization (MALDI) mass spectrometry and electrospray (ESI) tandem mass spectrometry on an Applied Biosystems Voyager-DE and a Finnigan LCQ instrument, respectively. A 0.5 μL aliquot of the sample (pepsin HPLC fraction or tryptic digest) was mixed 1:3 (v/v) with α-cyano-4-hydroxycinnamic acid matrix and 1 μL of the mixture allowed to dry on the sample plate. Typically, 250 laser shots were used to acquire a single MALDI mass spectrum. Spectra were calibrated externally with a mixture of angiotensin I (MW 1295) and bovine insulin (MW 5733). A custom nanospray source was used to infuse peptic or tryptic fragments into the LCQ instrument solubilized in water/acetonitrile/acetic acid (49/49/2 v/v/v). Tryptic digests were first desalted with C18 containing Zip-tips (Millipore). Ions generated by nanospray were detected and selected on the basis of their *m*/*z* ratio for subsequent fragmentation to produce sequence information.

Cloning, Expression, and Purification of PDE5/PDE6α′ Chimeras. The constructs for expression of Chi-GAFa and Chi-GAFb were obtained on the basis of the pFastBacHTb-Chi16 vector encoding for PDE5/PDE6α′ chimera, Chi16 (*22*). DNA fragments corresponding to amino acid sequences 335−661 and 4−334 of PDE5 were PCR-amplified using the pFastBacHTb-PDE5 vector as a template. The PCR products were cut with *Sac*I/*Nhe*I and *Sfo*I/*Sac*I, respectively, and subcloned into similarly digested pFastBacHTb-Chi16 to obtain Chi-GAFa and Chi-GAFb, respectively. Recombinant His_6-tagged chimeras were expressed in Sf9 cells and partially purified using affinity chromatography on a His-Bind resin (Novagen) as described earlier (*22*). Purified proteins were dialyzed against 40% glycerol and stored at −20 °C.

PDE Activity Assay. PDE activity was measured using 50−100 pM chimeric PDEs and [^{3}H]cGMP (0.5 μM) as substrate according to published procedures (*24*, *25*). Less than 15% of cGMP was hydrolyzed during these reactions. The K_i values were calculated by fitting the data to eq 1 in ref *26* with nonlinear least-squares criteria using GraphPad Prizm software.

RESULTS

Photo-Cross-Linking of Pγ-21−45Bpa^{23} to PDE6αβ. To identify the sites and residues on the PDE6 catalytic subunits that interact with the central polycationic region of Pγ, we designed synthetic peptides for cross-linking studies. Solid-phase peptide synthesis techniques allow the replacement of any amino acid in a peptide with photoactivatable amino acids. The most common and successful method has been

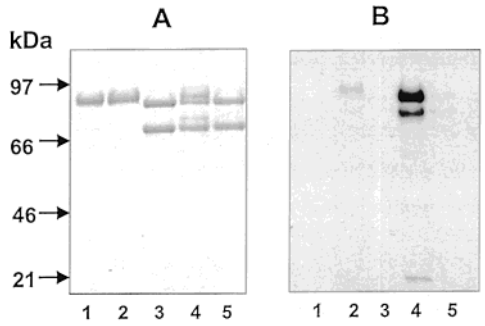

FIGURE 1: Cross-linking of Pγ-21−45Bpa^{23} to PDE6$\alpha\beta$. An SDS−PAGE gel (8%) stained with Coomassie Blue (A) and a Western blot with a streptavidin/horseradish peroxidase conjugate detection of the biotin-containing cross-linked products (B). Rod holoPDE6 (lanes 1 and 2) or trypsin-treated PDE6 (lanes 3−5) (2 μM each) was UV-irradiated in the absence (lanes 1 and 3) or in the presence of 10 μM Pγ-21−45Bpa^{23} (lanes 2 and 4) or in the presence of 10 μM Pγ and 10 μM Pγ-21−45Bpa^{23} (lane 5).

the use of *p*-benzoyl-L-phenylalanine (Bpa) as a photoactivatable replacement for aromatic or hydrophobic amino acid residues (*27*−*30*). Bpa is a benzophenone derivative, which is excited by UV light to a triplet biradical state. In the excited state, Bpa is highly reactive toward tertiary C−H bonds and unreactive toward water (*31*). Therefore, Bpa-containing peptides are often capable of producing high-yield cross-linking. Two peptides, Btn-NH-$(CH_2)_5$-CO-^{24}RKGP-PK*Bpa*KQRQTRQFKSKPPKK^{45}-NH_2 and Btn-NH-$(CH_2)_5$-CO-^{21}VT*Bpa*RK GPPKFKQRQTRQFKSKPPKK^{45}-NH_2, have been synthesized. In the first peptide corresponding to Pγ-24−45, Bpa replaced Phe^{30} of Pγ (Pγ-24−45Bpa^{30}). In the second peptide corresponding to Pγ-21−45, Bpa was inserted instead of PγPro^{23} (Pγ-21−45Bpa^{23}). Both peptides were biotinylated at the N-termini using biotin−aminohexanoic acid and amidated at the C-termini. The biotin tag served two functions. First, a Western blot analysis using a streptavidin/peroxidase conjugate allowed for monitoring for the presence of cross-linked products following various chromatographic procedures. Second, affinity chromatography using monomeric avidin was utilized to isolate cross-linked products. A cross-linking yield of ~35−45% was achieved between Pγ-24−45Bpa^{30} and PDE6$\alpha\beta$ (not shown). The P$\alpha\beta$/Pγ24−45Bpa30 cross-linked products were digested with Glu-C protease and subjected to chromatography on immobilized monomeric avidin. The major limitation was an incomplete digestion with Glu-C protease producing a complex mixture of relatively large peptides that were difficult to analyze by MS/MS mass spectrometry. A photo-cross-linking of Pγ-21−45Bpa^{23} to PDE6α was also very efficient with ~50% yield (Figure 1). The incorporation of Pγ-21−45Bpa^{23} into the 70 kDa PDE6β band was approximately 2-fold lower than that into the 88 kDa PDE6a band. However, the peptide was also cross-linked to the 20 kDa fragment of PDEβ. Apparently, the 70 and 20 kDa fragments are held together by intramolecular interactions in nondenatured preparations and are fully separated only on SDS gels (*20*). Therefore, the overall efficiency of cross-linking of Pγ-21−45Bpa^{23} to the α- and β-subunits appears to be comparable. No photoincorporation of the peptide into holoPDE6 or PDE6$\alpha\beta$ reconstituted with Pγ was observed, suggesting the specificity of cross-linking (Figure 1). These are important controls, as they demonstrate that there is no nonspecific incorporation of the peptide probe into PDE6$\alpha\beta$ sites not occupied by bound Pγ. The proximity of the photoprobe to the biotin tag in Pγ-21−45Bpa^{23} allowed a cleavage of the cross-linked products with proteases producing small fragments such as pepsin and trypsin.

Table 1: Summary of Observed Cross-Linked Products

obsd MW	cross-linked masses (Da) Pγ + PDEα(β)	sequence/ predicted MW
	Peptic Products	
3008	2547[a] + 461	α 138−142/461
3333[e]	2547[a] + 786	α 135−142/787
3482	2694[b] + 788	α 135−142/787
4272	3484[c] + 788	α 135−142/787
3754[e]	2547[a] + 1207	α 135−146/1207
3900	2694[b] + 1207	α 135−146/1207
	Peptic/Tryptic Products	
1426[e]	965[d] + 461	α 138−142/461
1752[e]	965[d] + 787	α 135−142/787
2171	965[d] + 1207	α 135−146/1207

[a] The mass of peptic product Pγ-21−37. [b] The mass of peptic product Pγ-21−38. [c] The mass of entire Pγ-21−45. [d] The mass of tryptic product Pγ-21−24. [e] Sequence confirmed by tandem mass spectrometry.

Identification of the Pγ-21−45Bpa^{23} Cross-Linking Site on PDE6α. Analysis of peptic fragments isolated by HPLC gave numerous signals by MALDI and ESI (Table 1). However, because of their size, sequencing of the cross-linked product by tandem mass spectrometry was prohibitive. Analysis of the major peptic and tryptic products of the Pγ-21−45Bpa^{23} peptide facilitated the interpretation of observed MALDI signals from peptic and peptic/tryptic digests. The major peptic products of Pγ-21−45Bpa^{23} corresponded to Pγ-21−37 (*m*/*z* 2547) and Pγ-21−38 (*m*/*z* 2694) while the major tryptic product corresponded to Pγ-21−24 (*m*/*z* 965). Subtraction of these peptide masses from putative cross-linked peptide molecular weights gave common PDE$\alpha\beta$ masses of 461, 787, and 1207 Da between the two digests. Subsequent sequence information obtained by tandem mass spectrometry allowed assignment of sequences of cross-linked PDEα peptides as summarized in Table 1.

The biotin tag gave a characteristic fragmentation pattern in the tandem mass spectrometry experiments, and this pattern was used to identify cross-linked peptides present in peptic or tryptic digests. This signature pattern is shown in the tandem mass spectrum (Figure 2) for the major tryptic fragment of the Pγ peptide Pγ-21−24Bpa^{23} (*m*/*z* 965). The fragment ions at 340, 411, 439, and 522 are predicted from the Pγ-21−24Bpa^{23} structure and are indicated on the structure shown at the top of the figure.

Tandem mass spectrometry of a cross-linked product after peptic and tryptic digestion revealed a cross-linked PDEα peptide corresponding to residues 138−142 (Figure 3). The signature biotin pattern is present at lower masses, and sequence information is present at larger masses. The data are consistent with the structure shown at the top of the figure with the cross-link at either Met^{138} or Gly^{139}. Other peptides corresponding to the same PDEα region were also sequenced, providing confirmatory evidence (summarized in Table 1). Furthermore, retrospective analysis of the larger peptic products allowed assignment of the cross-linked products shown in Table 1.

Pγ Inhibition of PDE5/PDE6α' Chimeras Containing PDE6γ' GAF Domains. To confirm the role of the GAFa

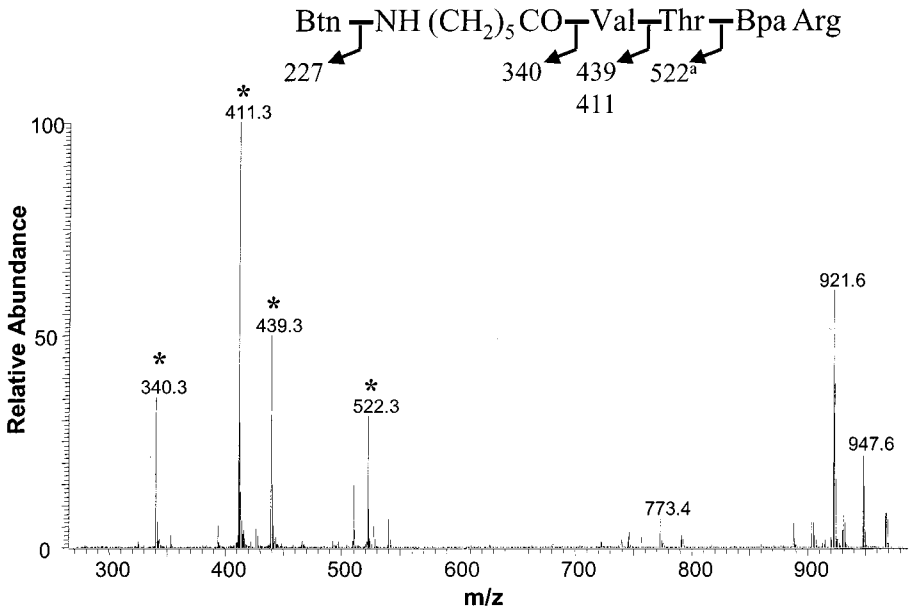

FIGURE 2: Tandem mass spectrum of the $[M + H]^+$ ion of the Pγ tryptic product at *m*/*z* 965. The biotin tag's signature ions are labeled with asterisks. The structure of the peptide with predicted fragment ion masses is shown above. [a]*m*/*z* 522 represents loss of water from the predicted fragment ion.

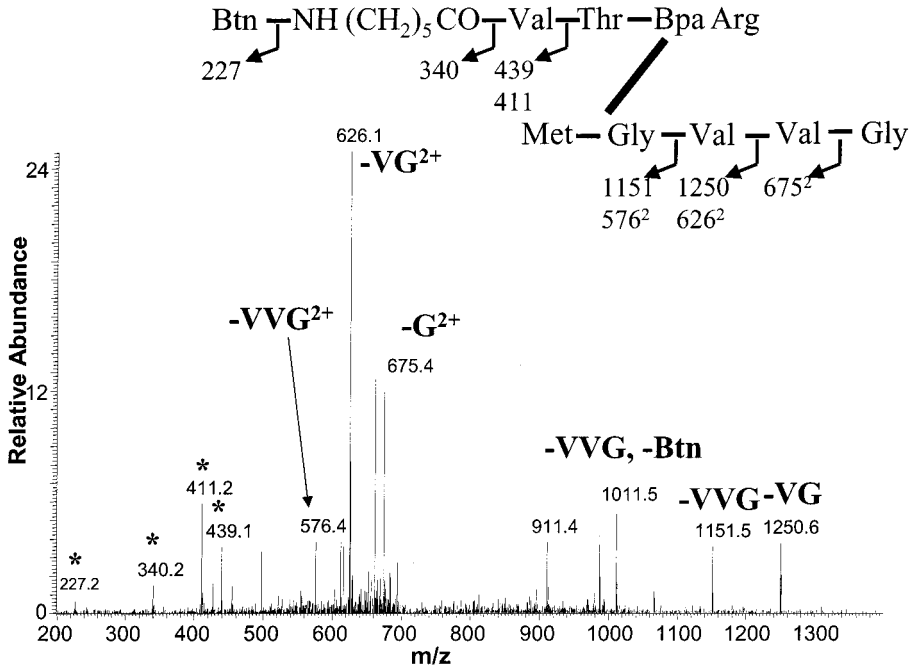

FIGURE 3: Tandem mass spectrum of the $[M + 2H]^{2+}$ ion of a cross-linked tryptic product at *m*/*z* 713 (MW 1426, Table 1). The biotin tag's signature ions are labeled with asterisks. Superscripts indicate the doubly charged ions observed.

domains and probe a potential role of the GAFb domains in the interaction of PDE6 catalytic subunits with Pγ, we constructed PDE5/PDE6α′ chimeras, Chi-GAFa and Chi-GAFb (Figure 4A), containing the PDE6α′ GAFa and GAFb domains, respectively. Chi-GAFa and Chi-GAFb have been examined for the inhibition by Pγ in comparison to previously generated Chi16 and Chi17 (*22*). Chi16 and Chi17 contain GAFa−GAFb domains from PDE6α′ and PDE5, respectively. Chi16, Chi17, Chi-GAFa, and Chi-GAFb all include the Pγ C-terminus binding site, PDE6α′-737−784, which enables these chimeras with the inhibitory interaction with Pγ (*22*). The K_i value (143 nM) and the maximal inhibition (65%) of Chi-GAFb by Pγ were similar to those for Chi17 (163 nM, 65%) (Figure 4B), suggesting that the GAFb domains do not significantly contribute to the interaction with Pγ. Consistent with the cross-linking data, Chi-GAFa was inhibited by Pγ more potently than Chi-GAFb or Chi17. Unlike Chi-GAFb and Chi17, Chi-GAFa was fully inhibited by Pγ with the K_i value of 44 nM. Yet, the K_i value for Chi-GAFa was notably higher than that for Chi16 (3.7 nM) (Figure 4B).

DISCUSSION

The inhibitory γ-subunit of PDE6 fulfills two functions in the PDE6 holoenzyme. The first and major task of Pγ is to block cGMP hydrolysis at the catalytic sites. The structural basis of this function has been recently elucidated. The C-terminal tail of Pγ directly binds to the perimeter of the

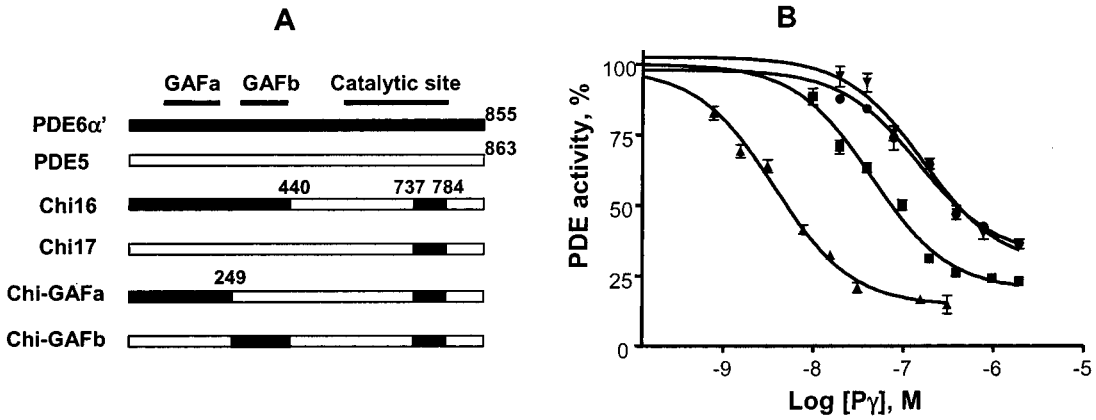

FIGURE 4: (A) Schematic representation of PDE6α′/PDE5 chimeras. (B) Inhibition of Chi16 (▲), Chi17 (▼), Chi-GAFa (■), and Chi-GAFb (●) by Pγ. PDE activities were measured upon addition of increasing concentrations of Pγ using 0.5 μM cGMP as substrate. The K_i values (nM) calculated from the inhibition curves were 3.7 ± 0.7 (▲), 163 ± 23 (maximal inhibition 65%) (▼), 44 ± 6 (■), and 143 ± 18 (maximal inhibition 65%) (●).

catalytic pocket and blocks the access of cGMP (*21*, *22*, *32*). The second and less understood role of Pγ is to stimulate binding of cGMP to the noncatalytic cGMP-binding sites formed by the PDE6 GAF domains (*13*−*15*). This function has been recently attributed to the polycationic, Lys/Arg-rich domain of Pγ (*8*, *9*). Apparently, the polycationic region of Pγ and the Pγ C-terminus only indirectly contribute to each other's primary roles by increasing the overall affinity of Pγ for PDE6 catalytic subunits. The sites of the Pγ polycationic region binding on PDE6 have not been fully investigated. A Pγ peptide, Pγ-24−45, was shown to bind a recombinant fragment of PDE6α, PDEα-461−553, corresponding to a region linking a second GAF domain (GAFb) with the catalytic domain (*33*). However, an estimated affinity of this interaction is approximately 3 orders of magnitude lower than that of the interaction between Pγ-24−45 and PDE6αβ, suggesting an important Pγ-24−45 binding epitope elsewhere on PDE6 (*33*). To identify this epitope, we have utilized a photo-cross-linking approach combined with identification of cross-linked site(s) by mass spectrometry. A specific high-yield cross-linking was achieved between a Bpa-containing peptide, Pγ-21−45Bpa[23], and PDE6αβ. The mass spectrometric analysis pointed to a single cross-linked site on PDE6α corresponding to residues Met[138]-Gly[139] located within the first GAF domain (GAFa). Methionine has been often reported as a site of cross-linking of benzophenone photoprobes (*28*, *30*). The chemical selectivity of benzophenone photoprobe cross-linking toward C−H bonds in several residues such Met, Leu, and Val (*27*−*31*) indicates that Met[138] is the cross-linked residue in PDE6α. A homology model of the PDE6α GAFa domain, generated using the coordinates of the PDE5 GAFa domain model (*12*), shows that Met[138] has high surface exposure and is readily accessible for the binding of Pγ-21−45 (Figure 5B). It should be noted, however, that the PDE6α GAFa model is not based on an experimentally solved structure of PDE5GAFa and, thus, should be considered as speculative. Although the site of Pγ-21−45Bpa[23] cross-linking to PDE6β has not been identified in this study, the cross-linking pattern suggests a similar region. The tryptic cleavage site producing the 70 and 20 kDa fragments of PDE6β corresponds to residues Lys[146]Lys[147](*20*). On the three-dimensional model of the PDE6α GAFa domain, residues both downstream and upstream of Lys[148]Lys[149] (PDE6β Lys[146]Lys[147]) are in close proximity to Met[138] (Figure 5B). The observed incorporation of Pγ-21−45Bpa[23] into both 70 and 20 kDa fragments of PDE6β is consistent with the cross-linking to residues adjacent to the tryptic site. The cross-linking of Pγ-21−45Bpa[23] to two or more residues of PDE6β may be due to the fact that the benzophenone-preferred methionine residue is substituted by Ile[136] in PDE6β (Figure 5A). The heterogeneity of PDE6β cross-linked products may have contributed to the failure of their identification using mass spectrometry.

The cross-linking results suggest a direct binding of Pγ-21−45Bpa[23] with the GAFa domains of PDE6. This interaction has been further supported by the analysis of inhibition of chimeric PDE5/PDE6α′ enzymes by Pγ. Chimeric PDE Chi-GAFa containing the PDE6α′ GAFa domain was inhibited by Pγ more potently than Chi-GAFb and Chi17 that had the GAFa and GAFa-GAFb domains of PDE5, respectively. The GAFa domains of photoreceptor PDEs are more homologous to each other (50−67% identity) than to PDE6GAFb (18−24% identity) or PDE5GAFa (30−32% identity) and are likely to contain specificity determinants for binding of Pγ-21−45 (Figure 5A). Comparable inhibition of Chi-GAFb and Chi17 by Pγ indicates that the PDE6GAFb domains are not directly involved in binding of Pγ. Nonetheless, PDE6GAFb appears to be important for the correct alignment of the Pγ C-terminus and the polycationic region with the PDE6 catalytic site and the GAFa domain, respectively. The electron microscopy and image analysis of PDE6 revealed the internal organization of each catalytic subunit into the three domains, GAFa, GAFb, and the catalytic domain, with GAFb situated between the other two domains (*34*). Improper alignment of the Pγ/PDE6α′ interaction sites due to the presence of PDE5GAFb in Chi-GAFa may account for the less effective inhibition by Pγ in comparison to Chi16. To reach both the catalytic domain and GAFa, Pγ would have to be in a stretched conformation. Alternatively, Pγ binding may induce significant conformational changes in PDE6 catalytic dimers that could draw the catalytic and GAFa domains closer to each other. A potential for large conformational changes in the GAF domain containing PDEs is highlighted by the effects of the N-terminal phosphorylation of PDE5 or noncatalytic cGMP binding to PDE2 on the PDE catalytic activity (*35*−*37*).

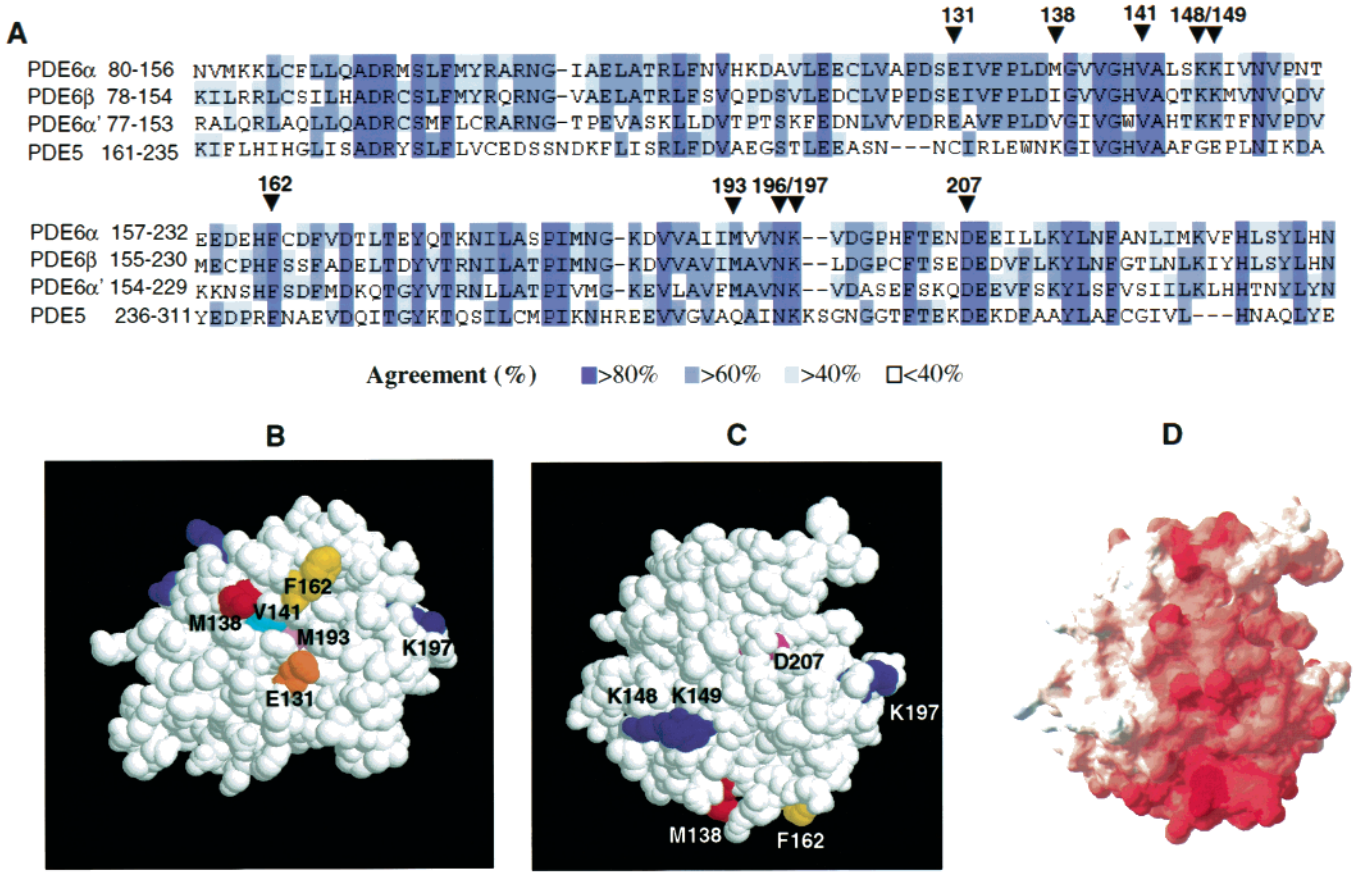

FIGURE 5: Model of the PDE6α GAFa domain. (A) An alignment (*41*) of PDE6 and PDE5 sequences corresponding to the GAFa domains (*11*, *42*). The arrows indicate the following: Met[138], the Pγ-21−45Bpa[23] cross-linked residue of PDE6α; Glu[131], Val[141], Phe[162], and Met[193] of PDE6α, counterpart residues to Cys[91], Cys[101], His[122], and Asp[149] from the Cys/His/Asp/Glu pocket of YKG9 (12); Asn[196], Lys[197], and Asp[207] from the NKX$_n$D cavity; and Lys[148]/Lys[149] corresponding to the tryptic cleavage site in PDE6*β* (*20*). (B and C) A model of the PDE6α GAFa domain was generated with the SWISS-MODEL (*43*) using the coordinates of the PDE5 GAFa model as a template (*12*). A space-filling representation of the model was obtained using RasMol (version 2.6). (B) A view of Met[138] and a cavity corresponding to the Cys/His/Asp/Glu pocket of YKG9 (*12*). (C) A view of Met[138] and the NKX$_n$D cavity. The orientation is rotated about the *X*-axis by 110° with respect to the view in (B). (D) The molecular surface of the PDE6α GAFa domain color-coded by electrostatic potential (−10 k_BT, red; +10 k_BT, blue) was generated using Swiss-PdbViewer (version 3.7b2). The orientation is the same as the view in (C).

What are the implications of our findings for the mechanism of potentiation of noncatalytic cGMP binding to the PDE6 GAF domains? The crystal structure of the GAF domain of *Saccharomyces cerevisiae* YKG9 protein revealed a buried pocket formed in part by three acidic residues, three Cys residues, and a His residue. A pocket corresponding to the Cys/His/Asp/Glu pocket of YKG9 is maintained in the GAF domains of phytochromes, where it is likely to serve as a ligand-binding site for tetrapyrrole (*12*). Furthermore, the GAF domain of YKG9 shows a remarkable similarity to the structures of PAS domains, another class of signal transduction modules (*12*, *38*). The PAS domains of photoactive yellow protein and histidine kinase FixL have cofactor-binding sites that coincide with the Cys/His/Asp/Glu pocket of YKG9 (*12*). By analogy with the PAS domains, the Cys/His/Asp/Glu pocket counterparts may be involved in noncatalytic cGMP binding by PDE GAF domains. Residues Glu[131], Val[141], Phe[162], and Met[193] corresponding to Cys[91], Cys[101], His[122], and Asp[149] from the YKG9 pocket are highlighted on the PDE6α GAFa model (Figure 5B). Met[138] adjoins these residues, suggesting that Pγ binds next to the "PAS-like pocket". If the PAS-like pocket represents a cGMP-binding site, the bound Pγ may directly stabilize cGMP contact residues on PDE6. Such stabilization would likely be reciprocal with the bound cGMP, providing for a more ordered Pγ-21−45 contact surface. Indeed, a 2.3-fold increase in the binding affinity of Pγ-1−45 for PDE6α*β* when the GAF domains are occupied by cGMP has been recently reported (*9*). An alternative site for noncatalytic cGMP binding to GAF domains is supported by mutagenesis of PDE5 (*39*, *40*), which demonstrated the key role of the NKX$_n$D motifs. The model of the PDE5 GAFa domain reveals a potential cGMP-binding pocket formed by the NKX$_n$D residues (*12*). On the PDE6α GAFa model, the pocket containing the motif residues N[196], K[197], and D[207] is at a significant distance (∼27−30 Å) from Met[138]. However, the surface adjacent to the Met[138]/PAS-like pocket and connecting them with the NKX$_n$D pocket is negatively charged (Figure 5C,D). Quite possibly, the positively charged polycationic region of Pγ takes advantage of favorable electrostatic interactions and binds to this surface. Consequently, the Pγ-21−45 binding site and the NKX$_n$D cavity might also be in close proximity.

Even though the finding of direct interaction of Pγ-21−45 with the PDE6 GAFa domain sheds a new light on the potential mechanism of positive cooperativity between the noncatalytic cGMP-binding sites and the Pγ-binding sites on PDE6, the question of a functional significance of this reciprocal regulation remains unresolved. A plausible hypothesis has been put forward. According to the hypothesis,

reductions in photoreceptor cGMP levels during visual transduction and/or light adaptation may lead to a state of low affinity of Pγ for PDE6 catalytic subunits, in which Pγ would become an effective cofactor in the RGS9 GAP function (*9*, *14*). Further studies are needed to determine if the occupancy of PDE6 GAF domains fluctuates during visual signaling and translates into the changes in Pγ binding that alter the activation/inactivation kinetics of phototransduction.

REFERENCES

1. Chabre, M., and Deterre, P. (1989) *Eur. J. Biochem. 179*, 255−266.
2. Yarfitz, S., and Hurley, J. B. (1994) *J. Biol. Chem. 269*, 14329−14332.
3. Li, T., Volpp, K., and Applebury, M. L. (1990) *Proc. Natl. Acad. Sci. U.S.A. 87*, 293−297.
4. Lipkin, V. M., Khramtsov, N. V., Vasilevskaya, I. A., Atabekova, N. V., Muradov, K. G., Gubanov, V. V., Li, T., Johnston, J. P., Volpp, K. J., and Applebury, M. L. (1990) *J. Biol. Chem. 265*, 12955−12959.
5. Hamilton, S. E., and Hurley, J. B. (1990) *J. Biol. Chem. 265*, 11259−11264.
6. Gillespie, P. G., and Beavo, J. A. (1988) *J. Biol. Chem. 263*, 8133−8141.
7. Gillespie, P. G., and Beavo, J. A. (1989) *Proc. Natl. Acad. Sci. U.S.A. 86*, 4311−4315.
8. Granovsky, A. E., Natochin, M., McEntaffer, R. L., Haik, T. L., Francis, S. H., Corbin, J. D., and Artemyev, N. O. (1998) *J. Biol. Chem. 273*, 24485−24490.
9. Mou, H., and Cote, R. H. (2001) *J. Biol. Chem. 276*, 27527−27534.
10. Shabb, J. B., and Corbin, J. D. (1992) *J. Biol. Chem. 267*, 5723−5726.
11. Aravind, L., and Ponting, C. P. (1997) *Trends Biochem. Sci. 22*, 458−459.
12. Ho, Y.-S. J., Burden, L. M., and Hurley, J. H. (2000) *EMBO J. 19*, 5288−5299.
13. Yamazaki, A., Bartucca, F., Ting, A., and Bitensky, M. W. (1982) *Proc. Natl. Acad. Sci. U.S.A. 79*, 3702−3706.
14. Cote, R. H., Bownds, M. D., and Arshavsky, V. Y. (1994) *Proc. Natl. Acad. Sci. U.S.A. 91*, 4845−4849.
15. Mou, H., Grazio, H. J., III, Cook, T. A., Beavo, J. A., and Cote, R. H. (1999) *J. Biol. Chem. 274*, 18813−18820.
16. Lipkin, V. M., Dumler, I. L., Muradov, K. G., Artemyev, N. O., and Etingof, R. N. (1988) *FEBS Lett. 234*, 287−290.
17. Artemyev, N. O., and Hamm, H. E. (1992) *Biochem. J. 283*, 273−279.
18. Brown, R. L. (1992) *Biochemistry 31*, 5918−5925.
19. Skiba, N. P., Artemyev, N. O., and Hamm, H. E. (1995) *J. Biol. Chem. 270*, 13210−13215.
20. Artemyev, N. O., Natochin, M., Busman, M., Schey, K. L., and Hamm, H. E. (1996) *Proc. Natl. Acad. Sci. U.S.A. 93*, 5407−5412.
21. Granovsky, A. E., Natochin, M., and Artemyev, N. O. (1997) *J. Biol. Chem. 272*, 11686−11689.
22. Granovsky, A. E., and Artemyev, N. O. (2000) *J. Biol. Chem. 275*, 41258−41262.
23. Papermaster, D. S., and Dreyer, W. J. (1974) *Biochemistry 13*, 2438−2444.
24. Thompson, W. J., and Appleman, M. M. (1971) *Biochemistry 10*, 311−316.
25. Natochin, M., and Artemyev, N. O. (2000) *Methods Enzymol. 315*, 539−554.
26. Granovsky, A. E., and Artemyev, N. O. (2001) *Biochemistry 40*, 13209−13215.
27. Kauer, J. C., Erickson-Viitanen, S., Wolfe, H. R., Jr., DeGrado, W. F. (1986) *J. Biol. Chem. 261*, 10695−10700.
28. Kage, R., Leeman, S. E., Krause, J. E., Costello, C. E., and Boyd, N. (1996) *J. Biol. Chem. 271*, 25797−25800.
29. Mills, J. S., Miettinen, H. M., Barnidge, D., Vlases, M. J., Wimer-Mackin, S., Dratz, E. A., Sunner, J., and Jesaitis, A. J. (1998) *J. Biol. Chem. 273*, 10428−10435.
30. Li, H., Macdonald, D. M., Hronowski, X., Costello, C. E., Leeman, S. E., and Boyd, N. D. (2001) *J. Biol. Chem. 276*, 10589−10593.
31. Dorman, G., and Prestwich, G. D. (1994) *Biochemistry 33*, 5661−5673.
32. Granovsky, A. E., and Artemyev, N. O. (2001) *J. Biol. Chem. 276*, 21698−21703.
33. Natochin, M., and Artemyev, N. O. (1996) *J. Biol. Chem. 271*, 19964−19969.
34. Kameni Tcheudji, J. F., Lebeau, L., Virmaux, N., Maftei, C. G., Cote, R. H., Lugnier, C., and Schultz, P. (2001) *J. Mol. Biol. 310*, 781−791.
35. Corbin, J. D., Turko, I. V., Beasley, A., and Francis, S. H. (2000) *Eur. J. Biochem. 267*, 2760−2767.
36. Rybalkin, S. D., Rybalkina, I. G., Feil, R., Hofmann, F., and Beavo, J. A. (2002) *J. Biol. Chem. 277*, 3310−3317.
37. Martins, T. J., Mumby, M. C., and Beavo, J. A. (1982) *J. Biol. Chem. 257*, 1973−1979.
38. Ponting, C. P., and Aravind, L. (1997) *Curr. Biol. 7*, R674−R677.
39. McAllister-Lucas, L. M., Haik, T. L., Colbran, J. L., Sonnenburg, W. K., Seger, D., Turko, I. V., Beavo, J. A., Francis, S. H., and Corbin, J. D. (1995) *J. Biol. Chem. 270*, 30671−30679.
40. Turko, I. V., Haik, T. L., McAllister-Lucas, L. M., Burns, F., Francis, S. H., and Corbin, J. D. (1996) *J. Biol. Chem. 271*, 22240−22244.
41. Thompson, J. D., Higgins, D. G., and Gibson, T. J. (1994) *Nucleic Acids Res. 22*, 4673−4680.
42. Schultz, J., Milpetz, F., Bork, P., and Ponting, C. P. (1998) *Proc. Natl. Acad. Sci. U.S.A. 95*, 5857−5864.
43. Guex, N., and Peitsch, M. C. (1997) *Electrophoresis 18*, 2714−2723.

BI015935M